The Influence of Anisotropic Membrane Inclusions on Curvature Elastic Properties of Lipid Membranes

Miha Fošnarič,[‡] Klemen Bohinc,[§] Dorit R. Gauger,[||] Aleš Iglič,[‡] Veronika Kralj-Iglič,*[,⊥] and Sylvio May[†,||]

Laboratory of Physics, Faculty of Electrical Engineering, University of Ljubljana, Tržaška 25, 1000 Ljubljana, Slovenia, UCHS, University of Ljubljana, Poljanska 26a, 1000 Ljubljana, Slovenia, Research Group "Lipid Membranes", Friedrich-Schiller University, Neugasse 25, Jena 07745, Germany, and Institute of Biophysics, Faculty of Medicine, University of Ljubljana, Lipičeva 2, 1000 Ljubljana, Slovenia

Received April 30, 2005

A membrane inclusion can be defined as a complex of protein or peptide and the surrounding significantly distorted lipids. We suggest a theoretical model that allows for the estimation of the influence of membrane inclusions on the curvature elastic properties of lipid membranes. Our treatment includes anisotropic inclusions whose energetics depends on their in-plane orientation within the membrane. On the basis of continuum elasticity theory, we calculate the inclusion-membrane interaction energy that reflects the protein or peptide-induced short-ranged elastic deformation of a bent lipid layer. A numerical estimate of the corresponding interaction constants indicates the ability of inclusions to sense membrane bending and to accumulate at regions of favorable curvature, matching the effective shape of the inclusions. Strongly anisotropic inclusions interact favorably with lipid layers that adopt saddlelike curvature; such structures may be stabilized energetically. We explore this possibility for the case of vesicle budding where we consider a shape sequence of closed, axisymmetric vesicles that form a (saddle-curvature adopting) membrane neck. It appears that not only isotropic but also strongly anisotropic inclusions can significantly contribute to the budding energetics, a finding that we discuss in terms of recent experiments.

INTRODUCTION

Biological membranes are multicomponent mixtures of lipids and associated biopolymers. They exhibit remarkable physical properties that have become a major focus of current research. Among those properties is the curvature elastic behavior of the underlying lipid matrix which has been recognized to be involved in various cellular processes such as vesicle budding, membrane fusion and fission, and pore formation. Moreover, the elastic properties of lipid membranes play a vital role in the lateral organization of membrane-associated biopolymers.

Various theoretical models are available to describe the elastic behavior either of single component or mixed membrane.[1,2] Membrane-inserted biopolymers, such as membrane-penetrating or integral proteins and amphipathic peptides, are sometimes represented as rigid membrane inclusions.[3] In this work, the term *membrane inclusion* is used for the membrane-inserted molecule and the surrounding lipids that are significantly distorted due to the presence of the inserted molecule.[4,5] The membrane-inserted molecule alone is referred to as the "rigid" core[6] of the inclusion (Figure 1).

The elastic nature of the host membrane has profound implications on the lateral organization of membrane inclusions. That is, short- or even long-range attraction between membrane inclusions may induce the formation of membrane domains.[8,9] Conversely, membrane inclusions may influence the conformation of the host membrane, a drastic example being the formation of nonbilayer phases induced by certain transmembrane proteins or peptides.[10]

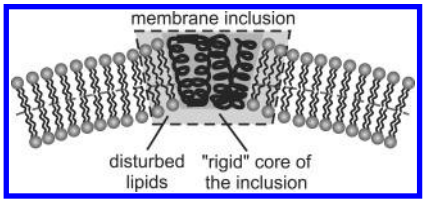

Figure 1. Schematic representation of the membrane inclusion (also called microdomain[7]). The membrane inserted molecule represents the "rigid" core of the inclusion. The surrounding lipids that are significantly distorted due to the presence of the core define the effective size of the membrane inclusion.

An interesting class of membrane inclusions are *anisotropic* inclusions. These inclusions interact with a curved membrane in an orientation-dependent manner. Alpha-helical amphipathic peptides and dimeric surfactants[11,12] and also certain membrane-penetrating proteins, lipids,[13,14] and lipoproteins[15] can be considered as possible realizations of anisotropic inclusions. There is some evidence for anisotropic inclusion-induced structural reorganization of lipid membranes, ranging from the formation of membrane nanotubes[11] to the stabilization of small pores in the lipid bilayer.[16−18]

Anisotropic inclusions are generally expected to favorably interact with regions of saddle-curvatures within lipid membranes.[19] Among the most apparent realizations of such

* Corresponding author: veronika.kralj-iglic@fe.uni-lj.si.
† Present address: Department of Physics, North Dakota State University, Fargo, ND 58105-5566.
‡ Faculty of Electrical Engineering, University of Ljubljana.
§ UCHS, University of Ljubljana.
|| Friedrich-Schiller University.
⊥ Faculty of Medicine, University of Ljubljana.

10.1021/ci050171t CCC: $30.25 © 2005 American Chemical Society
Published on Web 09/24/2005

structures is the formation of a membrane neck during the budding process of a closed vesicle.[5] In living cells it has been indicated that the formation of a bud is accompanied by lateral redistribution and subsequent accumulation of certain membrane components (both lipids and proteins) at highly and nonuniformly curved membrane regions.[20,21] The physical basis, namely the coupling between saddlelike membrane curvature and local composition of a mixed (that is, inclusion-containing) membrane, has recently received some attention.[5,22,23] It should be noted that, in addition to the accumulation of anisotropic membrane components at the saddlelike region of a membrane neck, the budding process may also be driven by the enrichment of (possibly isotropic) membrane components within the spherical region of a bud.[24−30] Both mechanisms may complement each other.

Recent theoretical work on anisotropic inclusions falls into two different categories. In the first, the "rigid" core of each individual inclusion imposes a defect in the membrane curvature field. The defects then serve as boundary conditions subject to which the membrane curvatures around the defect are optimized.[31−33] Note that here the inclusions interact via many-body forces, rendering the concurrent optimization of both the curvature field and the defects a nontrivial problem.[3] The second approach, used also in the present work, is based on the mean-field level. Here, at each local position, an ensemble of inclusions energetically interacts with a membrane of locally prescribed curvatures,[19,5] where the membrane curvatures act as an external field with which the inclusions interact. The curvature field and the lateral density of the inclusions are then determined self-consistently so as to minimize the overall free energy of the membrane.[34,35] The membrane-inclusion interaction energy is characterized by phenomenological interaction parameters whose magnitude dictates the lateral inclusion density and the corresponding membrane free energy.

The major goal of the present work is to provide estimates of these interaction constants and to analyze the consequences with respect to the ability of inclusions to migrate toward membrane regions of preferred curvatures. Besides focusing on isotropic inclusions we shall particularly focus on anisotropic inclusions and their potential to accumulate at regions of saddlelike curvature, including their energetic stabilization. Our estimates for the interaction constants allow us to argue that membrane components (like peptides or proteins), having a reasonably large degree of anisotropy, can be expected to sense and accumulate at saddlelike membrane curvatures if the curvatures fit those preferred by the inclusion.

We have organized our work as follows. The first subsection (*Free Energy*) of the section *Theoretical Model* recapitulates the (above-mentioned) mean-field approach of inclusion-membrane interactions and shows how to calculate the lateral distribution of anisotropic inclusions within a nonhomogeneously curved membrane, thereby taking into account the excluded volume effect that prevents unrealistically high local inclusion concentrations. Still in the first subsection we also introduce a structural criterion of anisotropic inclusions to be *strongly* anisotropic: they are able to render the Gaussian elastic modulus positive; see below. In the second subsection (*Microscopic Interaction Model*), we employ a microscopic model (which extends a recent work of Fournier[19]) to calculate estimates of the inclusion-membrane interaction constants. Based on that model, the third subsection (*Curvature-Induced Segregation of Inclusions*) further quantifies the degree of curvature-induced segregation of membrane inclusions. In the section *Vesicle Budding* we apply our model to a practical situation, namely to the budding of an axisymmetric closed vesicle, for which we compare the influence of isotropic and anisotropic inclusions. In the final section (*Discussion and Conclusions*), we discuss the relevance of our results and the approximations we have invoked.

THEORETICAL MODEL

Free Energy. We use the above-mentioned mean-field approach for the energetics of a lipid monolayer that contains anisotropic constituents. The underlying interaction model has been discussed previously[5,13,36] and will only shortly be summarized.

Consider a single molecular membrane constituent, which can either be a lipid or a membrane embedded biopolymer such as a protein, peptide, steroid, or surfactant. As introduced above, we define a membrane inclusion as the considered membrane constituent and some additional lipids (if any) that are significantly distorted due to the presence of the inclusion. Obviously, if the considered constituent is a lipid molecule, the inclusion is only this lipid molecule. However, some biopolymers might locally deform the surrounding membrane significantly, and then the effective radius of the inclusion can be (somewhat) larger than the actual radius of the biopolymer in the membrane.

To distinguish between different types of membrane components (inclusions) we assign to each species label i (with $i = 1, 2...$). The interaction of the membrane inclusion with the surrounding membrane gives rise to a free energy contribution E_i, which, generally, depends on both the curvature of the membrane and on the in-plane orientation of the molecule under consideration. The single-inclusion energy E_i reflects a mismatch between the local shape of the membrane and the intrinsic shape of the membrane inclusion. The curvature tensors describing the respective shapes are represented by diagonalized 2×2 matrices. The local curvature tensor is represented by $\mathbf{C}$ (with principal curvatures C_1 and C_2 as diagonal elements), and the intrinsic curvature tensor is represented by $\mathbf{C}_{m,i}$ (with principal curvatures $C_{1m,i}$ and $C_{2m,i}$ as diagonal elements). The corresponding principal axes systems are mutually rotated by an angle ω. The interaction energy $E_i = E_i(H, D)$ is obtained by expansion in terms of the invariants of the so-called mismatch tensor[37] represented by $\mathbf{M}_i = \mathbf{R}\mathbf{C}_{m,i}\mathbf{R}^{-1} - \mathbf{C}$, where $\mathbf{R}$ is the matrix describing the rotation by an angle ω. Taking into account terms up to the second order in curvature results in[5]

$$\frac{E_i}{kT} = (2K_i + \bar{K}_i)(H - H_{m,i})^2 - \bar{K}_i[D^2 - 2DD_{m,i}\cos(2\omega) + {D_{m,i}}^2] \quad (1)$$

where K_i and $\bar{K}_i$ are phenomenological constants, kT is the thermal energy, $H = (C_1 + C_2)/2$ is the mean curvature, and $D = (C_1 - C_2)/2$ denotes the curvature deviator.[38] The quantities $H_{m,i} = (C_{1m,i} + C_{2m,i})/2$ and $D_{m,i} = (C_{1m,i} - C_{2m,i})/2$ are the spontaneous mean and deviatoric curvatures that

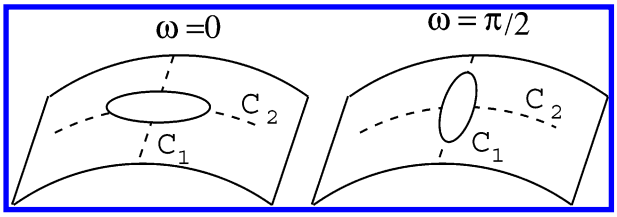

Figure 2. Two different orientations of an anisotropic membrane inclusion are schematically illustrated. They lead to minimal ($\omega = 0$) or maximal ($\omega = \pi/2$) interaction energy E_i (ω) with the host. Note that ω is the mutual rotation angle between the principal axes systems of the local curvature tensors of the membrane and the intrinsic curvature tensor of the inclusions. C_1 and C_2 denote the two principal curvatures of the lipid monolayer (for the sake of clarity, the case $C_1 = 0$ is displayed).

reflect the preferred local geometry of the membrane constituent. Maximum and minimum of E_i are adopted for mutual rotation angles $\omega = 0$ and $\omega = \pi/2$, respectively, as schematically illustrated in Figure 2.

Note that the curvature deviator $D_{m,i}$ describes the intrinsic anisotropy of the single membrane inclusion. Indeed, for $D_{m,i} = 0$ the ω-dependence of E_i disappears. Generally, the in-plane rotational degree of freedom of the membrane inclusion gives rise to a single-inclusion free energy f_i, which is obtained through statistical averaging over all available orientations ω; that is

$$\frac{f_i}{kT} = -\ln\left\{\frac{1}{2\pi}\int_0^{2\pi}\exp\left[-\frac{E_i(H, D) - E_i(0, 0)]}{kT}\right]d\omega\right\} \quad (2)$$

where we have chosen a planar membrane ($H = D = 0$) as the reference state for measuring f_i. We obtain

$$\frac{f_i}{kT} = (2K_i + \bar{K}_i)(H^2 - 2HH_{m,i}) - \bar{K}_i D^2 - \ln I_0(2\bar{K}_i D D_{m,i}) \quad (3)$$

where I_0 denotes the modified Bessel function.

Consider now a single (sufficiently large) lipid monolayer of lateral area A and local mean and deviatoric curvatures, H and D, respectively. The lipid monolayer is composed of two inclusion species, N_1 inclusions of type $i = 1$ and $N_2 = N - N_1$ inclusions of type $i = 2$ where N denotes the overall number of inclusions in the lipid monolayer (see also note 39). For the sake of simplicity we assume that both inclusions occupy the same lateral cross-sectional area $a = A/N$ per inclusion within the lipid monolayer. The fluidlike nature of the lipid layer allows its constituents to laterally redistribute. That is, in a nonhomogeneously curved lipid layer, the inclusions of both species are able to migrate toward their energetically preferred membrane regions so as to minimize the free energy (see note 40). We describe this degree of freedom by the local compositions, m_1 and $m_2 = 1 - m_1$, of the two species. Introducing the area average of any physical quantity Q via

$$\langle Q\rangle = \frac{1}{A}\int_A Q\, dA \quad (4)$$

we note the average compositions $\bar{m}_i = N_i/N = \langle m_i\rangle$. The free energy per inclusion F/N of the lipid monolayer contains both the single-inclusion free energies, f_i, and the corresponding demixing entropies

$$\frac{F}{N} = \left\langle \sum_{i=1}^{2} m_i f_i + kT\left(m_i \ln\frac{m_i}{\bar{m}_i} - m_i + \bar{m}_i\right)\right\rangle \quad (5)$$

In thermal equilibrium, F adopts its minimum with respect to the composition m_1 (or, equivalently, with respect to composition $m_2 = 1 - m_1$), subject to particle conservation, $\langle m_1\rangle = \bar{m}_1$. This results in the local composition

$$m_1 = \frac{e^{-(f_1 - f_2)/kT}}{\left\langle \frac{(1 - m_1)}{\bar{m}_1} e^{-(f_1 - f_2)/kT}\right\rangle + e^{-(f_1 - f_2)/kT}} \quad (6)$$

Obviously, for $f_1 = f_2$ there is no incentive for a segregation process, and we obtain $m_1 = \bar{m}_1$. Also, note the two limits, $f_1 \gg f_2$ implying $m_1 \to 0$, and $f_1 \ll f_2$ leading to $m_1 \to 1$.

If the lipid monolayer is composed of a single type of (lipid) molecule (say, component $i = 2$), then $m_1 = 0$, $m_2 = \bar{m}_2 = 1$, and the free energy is $F/N = \langle f_2\rangle$ where f_2 is given in eq 3 with $i = 2$. Note that the term $\ln I_0(2\bar{K}_2 D D_{m,2})$ describes the anisotropy of the lipids. Without an anisotropic contribution, F is equivalent to the familiar Helfrich bending energy[41] of a lipid layer with $\kappa = K_2 kT/a$ and $\bar{\kappa} = \bar{K}_2 kT/a$ being the bending stiffness and the Gaussian modulus, respectively. Even for small anisotropy, where $\ln I_0(x) = x^2/4$ with $x = |2\bar{K}_2 D D_{m,2}| \ll 1$, the free energy F remains quadratic in the curvatures with renormalized elastic moduli. As pointed out recently by Fournier,[19] the bending stiffness, $\kappa = [K_2 - (\bar{K}_2 D_{m,2})^2/2]kT/a$, decreases, whereas the Gaussian modulus, $\bar{\kappa} = [\bar{K}_2 + (\bar{K}_2 D_{m,2})^2]kT/a$, shifts to more positive values, the latter signifying a decreased stability with respect to the formation of saddlelike curvatures. It has been indicated recently[42] that the anisotropy of membrane lipids has implications on the shape and energetics of lipid membranes. It has been also suggested[13] to explain the stability of long cylindrical protrusions, emerging out of single-component phospholipid vesicles. Based on a minimization of the Helfrich-like bending energy, such cylindrical protrusions do not represent equilibrium shapes; they would rather form a chain of connected spherical microvesicles. Adding the contribution of anisotropy to the bending energy was shown to stabilize the cylindrical shape of the protrusions, that is observed in experiments.[13]

Consider now a two-component lipid monolayer, consisting of isotropic lipid molecules (inclusion species $i = 2$) and anisotropic inclusions (inclusion species $i = 1$). The isotropy of the lipid matrix implies $D_{m,2} = 0$, which we shall use in the following. As for a one-component lipid layer we can calculate for $|2\bar{K}_1 D D_{m,1}| \ll 1$ the effective elastic moduli, namely the bending stiffness, κ^{eff}, and the Gaussian modulus, $\bar{\kappa}^{\text{eff}}$. For a two-component lipid layer the elastic moduli will depend on the composition of the inclusions ($\bar{m}_1$). One may consider two different scenarios. In the first, the local composition $m_1 = \bar{m}_1$ is fixed for a given (small, and hence, uniformly curved) membrane patch. And in the second case, we allow for exchange of inclusions between the considered membrane patch and a planar bulk layer; in this case the chemical potential of the inclusions is fixed. Both scenarios lead to the same result for the bending stiffness[43]

$$\kappa^{\text{eff}} = \left\{\bar{m}_1\left[K_1 - \frac{1}{2}(\bar{K}_1 D_{m,1})^2\right] + (1 - \bar{m}_1)K_2\right\}\frac{kT}{a} \quad (7)$$

and also for the Gaussian modulus

$$\bar{\kappa}^{\text{eff}} = \{\bar{m}_1[\bar{K}_1 + (\bar{K}_1 D_{m,1})^2] + (1 - \bar{m}_1)\bar{K}_2\}\frac{kT}{a} \quad (8)$$

We see that both elastic moduli depend linearly on composition, which is a consequence of linearly combining the single-inclusion free energies in eq 5. Again, we clearly see the influence of the inclusion's anisotropy in downshifting κ^{eff} and upshifting $\bar{\kappa}^{\text{eff}}$. Obviously, for

$$\bar{K}_1 {D_{m,1}}^2 < -1 \quad (9)$$

and sufficiently large concentrations m_1 the Gaussian modulus $\bar{\kappa}^{\text{eff}}$ adopts a positive sign. We shall refer to inclusions that fulfill eq 9 as *strongly anisotropic* inclusions. Otherwise the inclusions are *weakly anisotropic*. Below, we investigate the ability of anisotropic inclusions to accumulate at (and to stabilize) regions of saddlelike curvature. As we shall see, only strongly anisotropic inclusions possess this ability.

Eq 6 takes into account saturation of m_1 for $f_1 \ll f_2$. Often however (and also relevant for the present work) the composition m_1 is sufficiently small everywhere so that the small composition limit ($m_1 \ll 1$) applies. From eq 6 we then obtain the Boltzmann distribution

$$\frac{m_1}{\bar{m}_1} = \frac{e^{-(f_1 - f_2)/kT}}{\langle e^{-(f_1 - f_2)/kT}\rangle} \quad (10)$$

and the corresponding free energy

$$\frac{F}{N} = \langle f_2\rangle - kT\bar{m}_1 \ln\langle e^{-(f_1 - f_2)/kT}\rangle \quad (11)$$

If in the small composition limit the (curved) lipid layer[44] is in contact with a reservoir of inclusions in the planar bulk membrane and the inclusions are allowed to exchange with this reservoir (of composition $\bar{m}_1^{\text{bulk}}$), we can re-express eq 11 as[36]

$$\frac{F}{N} = \langle f_2\rangle - kT(\bar{m}_1 - \bar{m}_1^{\text{bulk}}) \quad (12)$$

Here $N\bar{m}_1 = N\langle m_1\rangle$ is the actual number of inclusions residing in the (curved) lipid monolayer, and $N\bar{m}_1^{\text{bulk}}$ would be that number for $f_1 = f_2$. Differently expressed, $N(\bar{m}_1 - \bar{m}_1^{\text{bulk}})$ is the *excess* number of inclusions in the lipid monolayer, implying that each inclusion that migrates into the lipid layer from the bulk membrane lowers the free energy by 1 kT.

Microscopic Interaction Model. Here we suggest a microscopic interaction model for a mixed lipid monolayer that contains an anisotropic constituent. As above, we consider a two-component lipid layer ($i = 1, 2$). One component (labeled as inclusion species $i = 2$) is an isotropic lipid, and the other denotes the (anisotropic) inclusion species ($i = 1$). As discussed above, the interaction constants of the lipid host, $K_2 = a\kappa/kT$ and $\bar{K}_2 = a\bar{\kappa}/kT$, directly relate to the bending stiffness, κ, and Gaussian modulus, $\bar{\kappa}$, of the corresponding one-component lipid layer. We also assume that the lipids tend to assemble into a flat layer, implying $H_{m,2} = D_{m,2} = 0$.

The interaction constants of the anisotropic component (K_1, $\bar{K}_1$, $H_{m,1}$, and $D_{m,1}$) depend on its molecular structure. Our subject of interest in the present work are inclusions with rigid, anisotropic core (Figure 1), such as membrane-penetrating or transmembrane proteins (or peptides). Such proteins are anchored within the lipid layer through hydrophobic interactions. Owing to its softness, the hydrocarbon core of the host lipid layer can adjust to the shape of the (rigid) protein. The corresponding elastic lipid perturbation energy can be expected to depend on the curvature of the membrane. In fact, the curvature dependence determines the interaction constants, K_1, $\bar{K}_1$, $H_{m,1}$, and $D_{m,1}$, of the rigid inclusion with the host. In the following, we suggest a simple model to calculate the membrane-inclusion interaction constants, based on membrane elasticity theory.

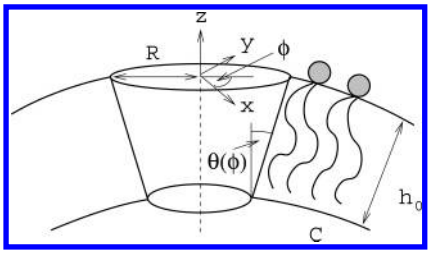

Figure 3. Schematic illustration of a rigid anisotropic core of the inclusion embedded in a lipid monolayer. The core of the inclusion is characterized by a "cone-angle" $\theta(\phi)$ that varies with the azimuthal angle ϕ. At the lipid headgroup region, the inclusion's core is circular with radius R. The curvature of the lipid monolayer, measured in radial direction, is $C(\phi)$. The equilibrium thickness of the monolayer's hydrocarbon core is h_0.

Consider a single, conelike, core of the inclusion that spans the host lipid monolayer as schematically illustrated in Figure 3.

To render the inclusion anisotropic we introduce a dependency of the cone angle $\theta = \theta(\phi)$ on the azimuthal angle ϕ; see Figure 3. For small variations of θ we can write

$$\theta(\phi) = \bar{\theta} + \Delta\theta \cos(2\phi) \quad (13)$$

where $\bar{\theta}$ is the average "coneness" of the core of the inclusion and $\Delta\theta$ is the corresponding deviator.

The core of the inclusion is embedded in a lipid monolayer of mean and deviatoric curvature H and D, respectively. Hence, according to the Lemma of Euler, the curvature measured in the radial direction of the inclusion, at the azimuthal angle ϕ, is

$$C(\phi) = H + D \cos(2\phi) \quad (14)$$

Formally, the inclusion-induced perturbation free energy, $f_1 = \int_L \tilde{f} dL = (L/2\pi)\int \tilde{f}(\phi)d\phi$, of the lipid monolayer can be expressed as an integration of the free energy density $\tilde{f}(\phi)$ per unit length of the circumference of the inclusion's core, $L = 2\pi R$, where R is the radius of the inclusion's core; see Figure 3. For a sufficiently large radius, R, we expect that $\tilde{f} = \tilde{f}[C(\phi),\theta(\phi)]$ depends only parametrically on ϕ, namely via the relations $C(\phi)$ and $\theta(\phi)$. More generally, $\tilde{f}$ should also depend on the derivatives of $C(\phi)$ and $\theta(\phi)$ with respect to ϕ. This additional dependence should become relevant if the radius R is smaller than the characteristic decay length ξ of membrane perturbations; below we estimate this length to be smaller than 1 nm. Hence, assuming that $R \geq \xi$ we can simply write

$$\frac{f_1}{L} = \frac{1}{2\pi}\int_0^{2\pi} \tilde{f}[C(\phi),\theta(\phi)]d\phi \tag{15}$$

In this case, $\tilde{f}$ can be calculated using a one-dimensional model for the elastic interaction of a lipid layer with an infinitely long, rigid wall. Such models have frequently been suggested in previous work,[45,46] and they can—as we show in the following—easily be generalized to a bent lipid layer of curvature C. Consider first a planar lipid monolayer, $C = 0$. The θ-dependence of $\tilde{f}$ can be written as a series expansion up to quadratic order

$$\tilde{f}(C=0,\theta) = \frac{\kappa}{2}\frac{1}{\xi}\theta^2 + C_0\theta \tag{16}$$

where κ is the bending stiffness of the lipid monolayer and C_0 is the spontaneous curvature. Using membrane elasticity theory, the characteristic length

$$\xi = h_0 \frac{\left(\sqrt{\frac{\kappa}{K}} + \frac{\kappa}{h_0\kappa_t}\right)}{\sqrt{2h_0\sqrt{\frac{\kappa}{K}} + \frac{\kappa}{\kappa_t}}} \tag{17}$$

has recently been calculated[46] for a planar ($C = 0$) lipid layer in contact with a wall tilted by an angle θ; it depends on the thickness of the lipid layer h_0, the lateral stretching modulus K, and the tilt modulus k_t. (In contrast to ref 46, no hydrophobic mismatch is included in eq 16.) Typically, for a lipid monolayer, $h_0 = 1.25$ nm, $\kappa \approx 10kT$, and $K \approx 20kT/\text{nm}^2$.[47] There is some uncertainty about the magnitude of the tilt modulus as it has never been determined experimentally. In the limit $k_t \ll K$ we obtain $\xi = (\kappa/k_t)^{1/2}$,[19] while $k_t \gg K$ yields $\xi = (h_0^2\kappa/(4K))^{1/4}$.[48] A recent molecular-level calculation[49] predicted $k_t = 20kT/\text{nm}^2$, just the same magnitude as the stretching modulus. It leads to $\xi = 0.9$ nm.

Let us generalize the result for the planar lipid monolayer (eq 16) to the bent one. This is achieved by applying the transformations $\theta \rightarrow \theta - CR$ and $C_0 \rightarrow C_0 - C$. The first transformation accounts for the rigidity of the inclusion's core, which cannot relax its shape upon bending. The second transformation represents the actual bending of the lipid monolayer. We obtain

$$\tilde{f}(C,\theta) = \frac{\kappa}{2\xi}(\theta - CR)^2 + (C_0 - C)(\theta - CR) \tag{18}$$

After inserting $\theta(\phi)$ from eq 13 and $C(\phi)$ from eq 14 into eq 18 and identifying ϕ with ω in eq 1 (for $i = 1$) we obtain

$$H_{m,1} = \frac{\bar{\theta}}{R}\left(\frac{R+\xi}{R+2\,\xi}\right) + \frac{\xi C_0}{R+2\,\xi},\; D_{m,1} = \frac{\Delta\theta}{R}\left(\frac{R+\xi}{R+2\,\xi}\right) \tag{19}$$

$$K_1 = \frac{3\pi\kappa}{4\,kT}R^2\left(\frac{R}{\xi}+2\right),\; \bar{K}_1 = -\frac{2}{3}K_1 \tag{20}$$

This is an important result of the present work on which our further discussion will be based. It confirms the expectation that the shape of the inclusion's core translates into a spontaneous mean curvature and spontaneous curvature deviator of order $H_{m,1} = \bar{\theta}/R$ and $D_{m,1} = \Delta\theta/R$, respectively. Note the strong dependence of the interaction constants K_1, $\bar{K}_1 \sim R^3$ on the core radius (for $R \gg \xi$); this is a consequence of both the rigidity of the inclusion core (contributing $\sim R^2$) and the linear increase of the circumference with R.

From eq 19 we can calculate the quantity $D_{m,1}\bar{K}_1 = -(\pi\kappa\Delta\theta R)\,(1 + R/\xi)/(2kT)$, which coincides (up to a numerical prefactor of order 1) with a recent estimate by Fournier (eq 5 in ref 19).

Curvature-Induced Segregation of Inclusions. The single-inclusion free energy depends on the curvature of the host layer, implying the possibility of a curvature-induced segregation of inclusions. In this case, the local composition of inclusions, m_1, varies over the lipid monolayer, as is quantified by eq 6. This equation somewhat simplifies if we consider equilibrium of a (sufficiently small) patch of (uniform) mean and deviatoric curvatures, H and D, respectively, with a large and flat ($D = H = 0$) membrane of inclusion composition $\bar{m}_1$. In this case, equality of the inclusion's chemical potential with that in the (planar) bulk membrane leads to the composition of inclusions at the curved membrane patch

$$m_1 = \frac{e^{-(f_1-f_2)/kT}}{\frac{1-\bar{m}_1}{\bar{m}_1} + e^{-(f_1-f_2)/kT}} \approx \bar{m}_1 e^{-(f_1-f_2)/kT} \tag{21}$$

where the last approximation refers to the small composition limit, $m_1 \ll 1$. Indeed, eq 21 follows directly from eq 6 as it is $f_1 = f_2 = 0$ everywhere at the flat membrane reservoir.

Below, we shall show that for reasonable estimates of the inclusion interaction parameters (given in eq 19) we expect $K_1 \gg K_2$ and $|\bar{K}_1| \gg |\bar{K}_2|$ (recall the sign of both $\bar{K}_1$ and $\bar{K}_2$ is negative.) In this case, on which we focus in the following, we simply have $f_1 - f_2 \approx f_1$ where f_1 is given in eq 3 (with $i = 1$).

At this point, we ask which curvatures are energetically most preferred by an inclusion. For strongly anisotropic inclusions (where $\bar{K}_1 D_{m,1}^2 < -1$) we may use the approximation $\ln I_0(x > 1) = x - \ln(2\pi x)/2$, and minimization of f_1 results in the optimal mean and deviatoric curvatures

$$H^{\text{opt}} = H_{m,1},\; D^{\text{opt}} = D_{m,1}\left(1 + \frac{1}{4\bar{K}_1 D_{m,1}^2}\right) \tag{22}$$

respectively, and in the corresponding free energy per inclusion

$$\frac{f_1 - f_2}{kT} = -(2K_1 + \bar{K}_1)H_{m,1}^2 + \bar{K}_1 D_{m,1}^2 + \frac{1}{16\bar{K}_1 D_{m,1}^2} + \frac{1}{2}\ln(-4\pi\bar{K}_1 D_{m,1}^2) \tag{23}$$

For weakly anisotropic inclusions the minimum of the deviatoric curvature is attained for $D^{\text{opt}} = 0$; hence, these inclusions do not tend to migrate toward favorably curved membrane regions.

In eq 22, the term $\sim 1/(\bar{K}_1 D_{m,1}^2)$ provides a correction to the strong coupling regime (where $D^{\text{opt}} = D_{m,1}$) attained for $|\bar{K}_1 D_{m,1}^2| \gg 1$. Because $\bar{K}_1 < 0$ this correction predicts $|D^{\text{opt}}| < |D_{m,1}|$. The preference for an optimal curvature deviator, D^{opt}, somewhat smaller than the spontaneous one is a consequence of the inclusion's in-plane orientational entropy.

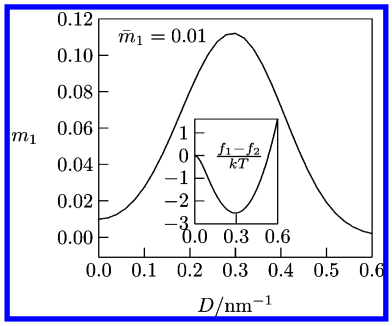

Figure 4. The composition m_1 as function of the saddle-curvature $D = C_1 = -C_2$ (with $H = 0$) for $\bar{m}_1 = 0.01$, calculated according to eq 21. The inset shows the corresponding $(f_1 - f_2)/kT$ for $\bar{K}_2 = -3$ nm^2, $\bar{K}_1 = -49$ nm^2, and $D_{m,1} = 1/3.4$ nm; see eq 3.

In the strong coupling regime where $\bar{K}_1 D_{m,1}^2 \ll -1$ we can disregard the last two terms in eq 23, the last term of it being only a weak logarithmic correction. Then, after inserting the expressions of eq 19 into eq 23, we obtain

$$\frac{f_1 - f_2}{kT} = -\frac{\pi\kappa}{kT}\left(\bar{\theta}^2 + \frac{1}{2}\Delta\theta^2\right)\frac{(R/\xi + 1)^2}{R/\xi + 2} \qquad (24)$$

which predicts an accumulation ($f_1 - f_2$ has negative sign) of inclusions in a region of a lipid monolayer that adopts the preferred curvatures $H = H^{\mathrm{opt}}$ and $D = D^{\mathrm{opt}}$. Equation 24 is a major result of the present work because it relates the energetic preference of an inclusion for an optimally bent lipid monolayer to the geometry (R, $\bar{\theta}$, and $\Delta\theta$) of that inclusion and to the elastic properties of the host layer (κ and ξ).

Let us estimate whether for a reasonable choice of the inclusion geometry we indeed obtain $|f_1 - f_2| \gg kT$ and $|f_1| \gg |f_2|$ as we have assumed in the derivation of eq 24. To that end, we assume for the sake of simplicity that a lipid monolayer is characterized by $H_{m,2} = D_{m,2} = 0$, a bending stiffness of $\kappa = 10\ kT$ and cross-sectional area per lipid $a = 0.6$ nm^2, leading to $K_2 = \kappa a/kT = 6$ nm^2. The Gaussian modulus is unknown for nearly all bare lipid membranes; yet there are indications to be of a smaller magnitude than the bending modulus. In fact, it was recently determined for the particular system of N-monomethylated dioleoylphosphatidylethanolamine to be $\bar{k}_1 = -0.82\kappa$.[50] Hence, we expect $0 > \bar{K}_2 > -6$ nm^2.

Next, we estimate the inclusion interaction parameters. We consider a saddlelike inclusion geometry (implying $\bar{\theta} = 0$; a nonvanishing $\bar{\theta}$ would further increase the magnitude of $f_1 - f_2$ in eq 24) with inclusion radius $R = 1.0$ nm and "cone"-angle variation $\Delta\theta = 0.44$ (corresponding to variations in the "cone"-angle within the region $\pm$ 25°). Based on eq 19 (with $\kappa = 10\ kT$ and $\xi = 0.9$ nm) we find $K_1 = 73$ nm^2, $\bar{K}_1 = -49$ nm^2, and $D_{m,1} = 1/3.4$ nm. These values are expected to be representative as helix tilt angles of even more than 25° are not uncommon for transmembrane proteins.[51]

Hence, our estimate confirms our assumptions, namely $K_1 \gg K_2$, $|K_1| \gg |\bar{K}_2|$, and also $D_{m,1}^2 \bar{K}_1 \ll -1$. In fact, for the latter we obtain $D_{m,1}^2 \bar{K}_1 = -4.2$, indicating strong orientational ordering of the anisotropic inclusions in a lipid monolayer of optimal (saddlelike) curvature.

As an illustration, Figure 4 shows $f_1 - f_2$ and the composition m_1 of the patch (see eq 21) as a function of the curvature deviator of the patch (D). The values of H and D are constant over the patch. The patch is in equilibrium with a large and flat membrane with inclusion composition $\bar{m}_1$, i.e. the chemical potential in the patch and in the bulk membrane are equal.

Transfer of each inclusion into the saddle-region of deviatoric curvature $D = D_{m,1}$ is accompanied by a gain for the single molecule free energy of about 2.5 kT, leading to a exp(2.5) ≈12-fold increase in the concentration of inclusions. The gain in overall free energy F (see eq 5, which includes the segregation-opposing demixing entropy of the inclusions) is 1kT per inclusion as is shown in eq 12.

VESICLE BUDDING

In this section we apply our considerations to the budding of bilayer vesicles. There are two possible scenarios of how inclusions can contribute to the energetics of bud formation.

The first concerns isotropic inclusions (where $D_{m,1} = 0$). These inclusions tend to migrate into the spherelike region of a bud. The fully developed bud consists essentially of a spherical vesicle to which the mother vesicle is connected via a small and highly curved neck. Let us assume that the inclusions are weakly cone-shaped, such that $(2K_1 + \bar{K}_1)H_{m,1}^2 \ll 1$ and where the radius of the bud, $R = 1/H_{m,1}$, allows an optimal interaction with the inclusions; see eq 22. The composition of inclusions in the bud is then $m_1 \approx \bar{m}_1 \exp[-(f_1 - f_2)/kT] \approx \bar{m}_1[1 + (2K_1 + \bar{K}_1)H_{m,1}^2]$. Note also the number of inclusions in the bud $N = 4\pi R^2 m_1/a$. From eq 12 we estimate that each inclusion that migrates toward the bud contributes a single kT to the free energy gain. The stabilization energy due to the migration of isotropic and (weakly) anisotropic inclusions is thus

$$\Delta F = -kT\frac{16\pi}{3a}\bar{m}_1 K_1 \qquad (25)$$

which is independent of the bud radius (and thus, independent of $H_{m,1}$). According to our numerical estimate above $K_1 = 73$ nm^2, implying that even at small compositions $\bar{m}_1$ the free energy gain $\Delta F \approx 2000\ \bar{m}_1 kT$ can be substantial even though the inclusions are weakly cone-shaped. In the case of more pronounced cone-shaped inclusions the effect can be much larger.

The second case is that of anisotropic inclusions. From the above analysis we know that only *strongly* anisotropic inclusions are expected to sense saddle-curvatures of lipid membranes. They tend to accumulate at regions of saddle-curvatures that roughly match the inclusion's spontaneous deviator. The membrane neck that connects a vesicle bud with the host exhibits pronounced saddle-curvatures. Here, we study the coupling between the nonhomogeneous lateral distribution of anisotropic membrane inclusions and membrane neck formation (see also note 52). To that end, we display in Figure 5 a well-known sequence of closed, axisymmetric vesicle shapes, starting from a pearlike shape proceeding to the limiting shape of two connected spherical vesicles.

The sequence was calculated as a function of the average mean curvature $\langle H \rangle$, at fixed area A and volume V of the closed vesicle. As is convenient, we express these quantities with respect to a spherical vesicle of radius R_s (and corresponding area $A_s = 4\pi R_s^2$ so that the relative area of each shape is normalized to $A_{\mathrm{rel}} = A/A_s = 1$). In Figure 5,

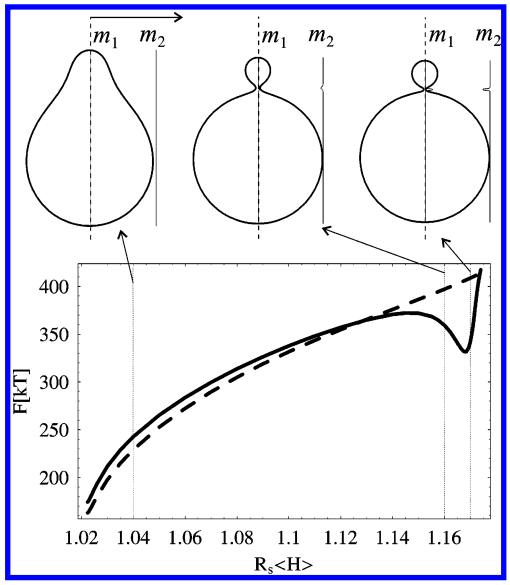

Figure 5. The free energy ΔF of the outer, anisotropic inclusion-containing monolayer (solid line) and the inner (inclusion-free) monolayer (broken line) of a closed vesicle, displayed as a function of increasing relative average mean curvature, $R_s\langle H\rangle$, for a sequence of axisymmetric pear shapes. Also shown are cross sections of three shapes, calculated for relative average mean curvature $R_s\langle H\rangle$: 1.04, 1.16, and 1.17, and the corresponding lateral distribution of anisotropic (m_1) and isotropic ($m_2 = 1 - m_1$) membrane components in the outer monolayer. The values of the parameters are as follows: $\bar{m}_1 = 0.01$ (0 for inner monolayer), $K_1 = 73$ nm^2, $\bar{K}_1 = -49$ nm^2, $H_{m,1} = 0$, $D_{m,1} = 1/(3.4$ nm), and for the host membrane $K_2 = 6$ nm^2, $\bar{K}_2 = -4$ nm^2, $H_{m,2} = D_{m,2} = 0$. Furthermore, it is $a = 0.6$ nm^2, $V_{rel} = 0.95$, and $R_s = 200$ nm.

the relative volume is $V_{rel} = 3V/4\pi R_s^3 = 0.95$ and $R_s = 200$ nm. Note that the mean curvature $\langle H\rangle$ is proportional to the area difference between the outer and inner monolayer ΔA (if the distance between the two monolayers (δ) is sufficiently small). Hence, the *relative* average mean curvature $R_s\langle H\rangle$ measures the relative area difference between the two monolayers relative to that of a spherical vesicle of radius R_s ($R_s\langle H\rangle = \Delta A_{rel} = \Delta A/8\pi\delta R_s$). We have chosen $R_s\langle H\rangle$ as our "reaction coordinate" with respect to which the energy of the vesicle is displayed as $\langle H\rangle$ can be manipulated experimentally by changing the temperature or by inserting additional molecules into one of the two monolayers.

The shape sequence in Figure 5 is computed for an inclusion-free vesicle, based on a minimization of the Helfrich free energy as explained elsewhere.[53] Here we use that sequence to estimate the influence of inclusions on the energetics of budding. To that end, we consider the presence of inclusions only in the *outer* monolayer, while the *inner* monolayer remains inclusion-free. Thereby we assume that the presence of inclusions does not affect the vesicle shapes. This assumption is justified by the small concentration, $\bar{m}_1 = 0.01$, of inclusions in the outer monolayer. Note that a solution of the full shape equations (those taking into account the coupling between the bending energy and the local monolayer composition self-consistently) can only lead to a lower free energy F than predicted by our approach. That would even more underline the role of anisotropic inclusions for stabilizing saddle-shaped vesicle necks than Figure 5 already does.

Figure 5 shows the free energies (F) of the outer (solid line) and inner (broken line) monolayer[54] of the two-component membrane for $\bar{m}_1 = 0.01$ (see also note 54). The inclusions are assumed to be of saddlelike geometry with interaction parameters as specified in the last section, namely, $K_1 = 73$ nm^2, $\bar{K}_1 = -49$ nm^2, $D_{m,1} = 1/3.4$ nm, $H_{m,1} = 0$. The properties of the host membrane (again as discussed in the previous section) are $H_{m,2} = D_{m,2} = 0$, $K_2 = 6$ nm^2, and $\bar{K}_2 = -4$ nm^2.

The free energy of the *inner* monolayer (broken line in Figure 5) increases *monotonically* from somewhat more than the single sphere value $F \approx 4\pi kT(2K_2 + \bar{K}_2)/a \approx 170\ kT$ to that of two connected spheres $F \approx 4\pi kT(4K_2 + \bar{K}_2)/a \approx 420\ kT$. In contrast to that, the free energy of the outer inclusion-containing monolayer of the pear-shaped vesicle has a pronounced minimum for a specific shape of the vesicle with a thin neck. The saddlelike curvatures of that neck indeed match the ones preferred by the anisotropic inclusions. The magnitude of inclusion accumulation at these regions (which is also displayed in Figure 5) corresponds to the prediction in Figure 4. While the outer monolayer of the vesicle contains about $4\pi R_s^2\bar{m}_1/a \approx 8000$ inclusions, only about 1% of them accumulate at the neck region where they induce an energetic gain for ΔF of about 1 kT per inclusion.

Accumulation of anisotropic inclusions in the necklike curved region of the bud has already been proposed before.[5,23] For example, dynamins (cytosol proteins playing a key-role in clathrin-mediated endocytosis) partly insert within the membrane and seem to accommodate cylindrical (anisotropic) curvature. Fournier et al.[23] indicated that the coupling between dynamins and the necklike curved membrane of the clathrin bud can result in a dynamin collar around the neck of the bud.

Various kinds of inclusion-induced vesicle shape transformations have recently been observed experimentally. Among them is the formation of lipid nanotubes induced by certain synthetic alpha-helical, amphipathic peptides.[55,56] These peptides have a cylinderlike shape and partially insert into the membrane with their long axis being parallel to the membrane plane, rendering them anisotropic (with $C_{1m,1} = 0$ and $C_{2m,1} \neq 0$). Inducing tubular vesicles through the coupling of their cylinderlike shape with the actual membrane shape is one application of the present work; see also refs 19 and 11. It appears that another (synthetic, amphipathic, and positively charged) peptide, called peptide-1, has the ability to induce budding or to drive a pearling instability of a cylindrical vesicle.[57] The corresponding mechanism is likely to be a peptide adsorption-induced increase of the relative area difference between the two monolayers (or, equivalently, an increase in $R_s\langle H\rangle$ as shown in Figure 5). However, the energetics of the budding (or pearling) process as well as the spatial distribution of the peptides on the bent vesicle could significantly be affected by the degree of peptide anisotropy.

DISCUSSION AND CONCLUSIONS

The interaction between a single inclusion and a membrane of prescribed curvatures is characterized by a number of phenomenological interaction constants. These interaction constants reflect a local structural perturbation of the membrane in the vicinity of the inclusion's core. Estimates of the interaction constants are derived based on a simple microscopic model, similar to the one suggested by Fourn-

ier.[19] The corresponding results (see eqs 19), together with the expression for the inclusion free energy (eq 24), constitute the major results of the present work and provide a complete energetic description of the inclusion-containing membrane up to the second order in curvatures. To illustrate the consequences that the presence of anisotropic inclusions can have one the conformation of a membrane, we have studied the budding of an axisymmetric closed vesicle for which we find a strong stabilization of the bud.

In our model the membrane inclusion consists of a rigid core and the surrounding lipids that are significantly distorted due to the presence of this core (Figure 1). If the local distortion of the lipids around the core propagates far into the membrane, the effective size of the whole inclusion can be significantly larger than that of the core. In this case the presented lattice statistics approach with the assumption of equal lattice sites for all membrane components can no longer be justified.[58] However, such long-ranged relaxations around a rigid inclusion core are often suppressed by additional constraints. For example, for closed membrane shapes, the fixed numbers of molecules in both membrane monolayers and the fixed volume of the cell (vesicle) determine the overall shape of the membrane[59,60] and thus greatly reduce the local relaxation of the membrane shape around the core of an inclusion. Extreme examples are (nearly) spherical vesicles or the vesicles with shapes close to the limiting shapes composed of a spherical mother vesicle and spherical daughter vesicles (see Figure 4 in section 2). In addition, the local membrane stress imposed by the inclusion's core can be partially relaxed by the accumulation of hydrophobic solutes in the hydrophobic region of lipid tails.[61] One should also bear in mind that there exist various types of (semi-flexible) membrane inclusions, which may disturb the membrane in a very different way than the rigid core of the inclusion considered in section 3. Namely, due to specific lipid−protein interactions and their intrinsic shapes the preferential clustering of lipids and proteins[62] may result in the formation of small protein−lipid membrane complexes,[63] which may be considered as membrane inclusions.[35] A typical example of such protein−lipid membrane inclusions are lipid−prominin complexes composed of the membrane-spanning domains of the protein prominin and the intermediate space being filled with cholesterol and other lipids. In accordance with our theoretical predictions anisotropic prominin inclusions are predominantly accumulated on highly curved membrane protrusions.[64]

With complex interactions between proteins and/or lipids also larger and more complex structures can form. For example, anion-exchange protein band-3 might form a core of a macrocomplex of red blood cell proteins.[65] Also, conformational changes of the same protein might mediate shape changes of the human red blood cell.[66]

Most of the previous work on inclusions in curved membranes predicts complex behavior concerning the lateral organization of the inclusions. However, as in the present work, *direct* interactions between inclusions are usually neglected; their consideration would add another level of complexity. On the other hand, they can be expected to act in almost every composed lipid membrane, arising typically from electrostatic, steric, or hydrophobic interactions. It is thus interesting to ask how their presence would affect the predictions of the present work. Recall that anisotropic inclusions—even in the absence of direct interactions—tend to migrate from planar into saddlelike membrane regions, the extent of which is dictated by the difference in the inclusion's standard chemical potential $f_1 - f_2$; see eq 21. Clearly, direct interactions between inclusions amplify this behavior. That is, if inclusions effectively attract (repel) each other, the migration toward the saddlelike region is enhanced (diminished). Note that this amplification is partially opposed by the loss of translational entropy associated with changes in the local inclusion concentration within the membrane. A mathematical treatment can be based on the mean-field level of regular solution theory which would add to the free energy per molecule of the lipid layer (eq 5) two additional terms; one quadratic in the composition of inclusions[34] and another one quadratic in the gradient of the composition. Note that ultimately, for sufficiently strong attractive interactions between the inclusions, lateral phase separation will take place, which too may couple to the membrane shape.[67] Although our approach suffers from neglecting direct interactions and correlations between inclusions, it offers computational advantages that allow us to employ it for modeling of various experimental observations, like vesicle budding (section 3) or the formation of stable lipid nanotubular protrusions[13,68] and membrane pores.[36]

To summarize, our results support and quantify the notion of a coupling between the lateral distribution of membrane inclusions and the membrane curvature. We expect that some membrane proteins or peptides, if they exhibit conelike or saddlelike shape (for example, due to a bundle of tilted transmembrane helices), are able to migrate toward a favorably curved membrane region or to induce the formation of such regions. The present work has focused on saddlelike membrane inclusions which favorably interact with saddlelike membrane curvatures; yet, a similar reasoning is valid for the migration of cone-shaped proteins toward membrane regions of spherelike curvature, occurring in caveolae or budding regions. Most notably, membrane inclusions are expected to significantly contribute to the energy required to form a curved membrane region. For example, as we suggest in section 3, the budding of a vesicle can be supported by lowering the energy of its neck via saddlelike inclusions.

ACKNOWLEDGMENT

S.M. and D.R.G. thank the TMWFK. A.I. appreciates support via a DAAD grant. M.F., V.K.I., A.I., and K.B. thank the Ministry of Science of the Republic of Slovenia for financial support.

REFERENCES AND NOTES

(1) Safran, S. A. Curvature elasticity of thin films. *Adv. Phys.* **1999**, *48*, 395−448.

(2) Ben-Shaul, A. Molecular theory of chain packing, elasticity and lipid protein interaction in lipid bilayers. In *Structure and Dynamics of Membranes*; Lipowsky, R., Sackmann, E., Eds.; Elsevier: Amsterdam, 1995; Vol. 1.

(3) Dommersnes, P. G.; Fournier, J. B. The Many-Body Problem for Anisotropic Membrane Inclusions and the Self-Assembly of "Saddle" Defects into an "Egg Carton". *Biophys. J.* **2002**, *83*, 2898−2905.

(4) Marčelja, S. Chain Ordering in Liquid Crystals II. Structure of bilayer membranes. *Biophys. Biochim. Acta* **1974**, *367*, 165−176.

(5) Kralj-Iglič, V.; Heinrich, V.; Svetina, S.; Žekš, B. Free energy of closed membrane with anisotropic inclusions. *Eur. Phys. J. B* **1999**, *10*, 5−8.

(6) Bruce, L. J.; Beckmann, R.; Ribeiro, M. L.; Peters, L. L.; Chasis, J. A.; Delaunay, J.; Mohandas, N.; Anstee, D. J.; Tanner, M. J. A band 3-based microcomplex of integral and peripheral proteins in the RBC membrane. *Blood* **2003**, *101*, 4180−4188.

(7) Brown, D. A.; London, E. Structure and Origin of Ordered Lipid Domains in Biological Membranes. *J. Membr. Biol.* **1998**, *164*, 103−114.

(8) Goulian, M. Inclusions in membranes. *Curr. Opin. Colloid Interface Sci.* **1996**, *1*, 358−361.

(9) Kim, K. S.; Neu, J.; Oster, G. Many-body forces between membrane inclusions: A new pattern formation mechanism. *Europhys. Lett.* **1999**, *48*, 99−105.

(10) Killian, J. A. Hydrophobic mismatch between proteins and lipids in membranes. *Biophys. Biochim. Acta* **1998**, *1376*, 401−416.

(11) Kralj-Iglič, V.; Iglič, A.; Hägerstrand, H.; Peterlin, P. *Phys. Rev. E* **2000**, *61*, 4230−4234.

(12) Marques, C. M.; Fournier, J. B. *Europhys. Lett.* **1996**, *35*, 361−365.

(13) Kralj-Iglič, V.; Iglič, A.; Gomišček, G.; Sevšek, F.; Arrigler, V.; Hägerstrand, H. Stable tubular microexovesicles of the erythrocyte membrane induced by dimeric amphiphiles. *J. Phys. A: Math. Gen.* **2002**, *35*, 1533−1549.

(14) Chanturiya, A.; Yang, J.; Scaria, P.; Stanek, J.; Frei, J.; Mett, H.; Woodle, M. New Cationic Lipids Form Channel-Like Pores in Phospholipid Bilayers. *Biophys. J.* **2003**, *84*, 1750−1755.

(15) Malev, V. V.; Schagina, L. V.; Gurnev, P. A.; Takemoto, J. Y.; Nestorovich, E. M.; Bezrukov, S. M. Syringomycin E channel: A lipidic pore stabilized by lipopeptide? *Biophys. J.* **2002**, *82*, 1985−1994.

(16) Matsuzaki, K. Magainins as paradigm for the mode of action of pore forming polypeptides. *Biochim. Biophys. Acta* **1998**, *1376*, 391−400.

(17) Kandušer, M.; Fošnarič, M.; Šentjurc, M.; Kralj-Iglič, V.; Hägerstrand, H.; Iglič, A.; Miklavčič, D. Effect of surfactant polyoxyethylene glycol (C12E8) on electroporation of cell line DC3F. *Colloid Surf., A* **2003**, *214*, 205−217.

(18) Pavlin, M.; Kandušer, M.; Reberšek, M.; Pucihar, G.; Hart, F. X.; Magjarević, R.; Miklavčič, D. Effect of Cell Electroporation on the Conductivity of a Cell Suspension. *Biophys. J.* **2005**, *88*, 1−13.

(19) Fournier, J. B. Nontopological saddle-splay and curvature instabilities from anisotropic membrane inclusions. *Phys. Rev. Lett.* **1996**, *76*, 4436−4439.

(20) H. Sprong, P. v. d. S.; van Meer, G. How proteins move lipids and lipids move proteins. *Nat. Cell. Biol.* **2001**, *2*, 504−513.

(21) J. C. Holthuis, G. v. M.; Huitema, K. Lipid microdomains, lipid translocation and the organization of intracellular membrane transport (Review). *Mol. Membr. Biol.* **2003**, *20*, 231−241.

(22) Shemesh, T.; Luini, A.; Malhotra, V.; Burger, K. N. J.; Kozlov, M. M. Prefission Constriction of Golgi Tubular Carriers Driven by Local Lipid Metabolism: A Theoretical Model. *Biophys. J.* **2003**, *85*, 3813−3827.

(23) Fournier, J. B.; Dommersnes, P. G.; Galatola, P. Dynamin recruitment by clathrin coats: a physical step? *C. R. Biologies* **2003**, *326*, 467−476.

(24) Lipowsky, R. Budding of membranes induced by intramembrane domains. *J. Phys. II (France)* **1992**, *2*, 1825−1840.

(25) Kawakatsu, T.; Andelman, D.; Kawasaki, K.; Taniguchi, T. Phase transitions and shapes of two component membranes and vesicles I: strong segregation limit. *J. Phys. II (France)* **1993**, *3*, 971−997.

(26) Hägerstrand, H.; Isomaa, B. Lipid and protein composition of exovesicles released from human erythrocytes following treatment with amphiphiles. *Biochim. Biophys. Acta* **1994**, *1190*, 409−415.

(27) Julicher, F.; Lipowsky, R. Shape transformations of vesicles with intramembrane domains. *Phys. Rev. E* **1996**, *53*, 2670−2683.

(28) Kumar, P. B. S.; Gompper, G.; Lipowsky, R. Budding Dynamics of Multicomponent Membranes. *Phys. Rev. Lett.* **2001**, *86*, 3911−3914.

(29) Lipowsky, R.; Dimova, R. Domains in membranes and vesicles. *J. Phys.: Condens. Matter* **2003**, *15*, S31−S45 Sp. Iss. SI JAN 15 2003.

(30) Laradji, M.; Kumar, P. B. S. Dynamics of Domain Growth in Self-Assembled Fluid Vesicles. *Phys. Rev. Lett.* **2004**, *93*, 198105.

(31) Kim, K. S.; Neu, J.; Oster, G. Effect of protein shape on multibody interactions between membrane inclusions. *Phys. Rev. E* **2000**, *61*, 4281−4285.

(32) Dommersnes, P. G.; Fournier, J. B. N-body study of anisotropic membrane inclusions: Membrane mediated interactions and ordered aggregation. *Eur. Phys. J. B* **1999**, *12*, 9−12.

(33) Chou, T.; Kim, K. S.; Oster, G. Statistical Thermodynamics of Membrane Bending-Mediated Protein−Protein Attractions. *Biophys. J.* **2001**, *80*, 1075−1087.

(34) Markin, V. S. Lateral organization of membranes and cell shapes. *Biophys. J.* **1981**, *36*, 1−19.

(35) Iglič, A.; Fošnarič, M.; Hägerstrand, H.; Kralj-Iglič, V. Coupling between vesicle shape and the nonhomogeneous lateral distribution of membrane constituents in Golgi bodies. *FEBS Lett.* **2004**, *574*, 9−12.

(36) Fošnarič, M.; Kralj-Iglič, V.; Bohinc, K.; Iglič, A.; May, S. Stabilization of pores in lipid bilayers by anisotropic inclusions. *J. Phys. Chem. B* **2003**, *107*, 12519−12526.

(37) Kralj-Iglič, V.; Remškar, M.; Vidmar, G. Fošnarič, M.; Iglič, A. Deviatoric elasticity as a possible physical mechanism explaining collapse of inorganic micro and nanotubes. *Phys. Lett. A* **2002**, *296*, 151−155.

(38) Strictly speaking, the curvature deviator (which is an invariant of the curvature tensor) is defined as $D = |C_1 - C_2|/2$. However, we can choose C_1 and C_2 in such a way that it is always $C_1 > C_2$.

(39) Although the term *inclusion species* is quite general at this point, we have in mind the more specific situation (that is also used later in the text) where inclusion species $i = 2$ denotes lipid molecules and species $i = 1$ are the actual inclusions embedded in the lipid monolayer.

(40) The lateral redistribution of membrane constituents can also affect the shape of the membrane. Yet, this degree of freedom can be taken into account in a later step where one allows for the variation of the membrane shape (with equilibrated inclusion distribution).

(41) Helfrich, W. Elastic properties of lipid bilayers: theory and possible experiments. *Z. Naturforsch.* **1973**, *28*, 693−703.

(42) Kralj-Iglič, V.; Babnik, B.; Gauger, D. R.; May, S.; Iglič, A. Quadrupolar Ordering of Phospholipid Molecules in Narrow Necks of Phospholipid Vesicles. *J. Stat. Phys.* **2005**, in press.

(43) As for the one-component membrane, also the free energy F of the two-component membrane remains for small anisotropies quadratic in the curvatures because $\ln I_0(x) = x^2/4$ for $x = |2\bar{K}_2 D D_{m,2}| \ll 1$. Therefore, for fixed local composition $m_1 = \bar{m}_1$, one obtains the effective elastic moduli directly by comparing the expression for the free energy with the familiar Helfrich bending energy. The case of fixed chemical potential of the inclusions yields the same result for the effective elastic moduli.

(44) Here the expression *(curved) lipid layer* is used for a region of the lipid layer with given curvature (in contrast to a *planar bulk membrane* that serves as a reservoir of inclusions).

(45) Dan, N.; Safran, S. A. Effect of lipid characteristics on the structure of transmembrane proteins. *Biophys. J.* **1998**, *75*, 1410−1414.

(46) May, S. Membrane Perturbations Induced by Integral Proteins: Role of Conformational Restrictions of the Lipid Chains. *Langmuir* **2002**, *18*, 6356−6364.

(47) Safinya, C. R.; Sirota, E. B.; Roux, D.; Smith, G. S. Universality in interacting membranes: The effect of cosurfactants on the interfacial rigidity. *Phys. Rev. Lett.* **1989**, *62*, 1134−1137.

(48) Harroun, T. A.; Heller, W. T.; Weiss, T. M.; Yang, L.; Huang, H. W. Theoretical analysis of hydrophobic matching and membrane-mediated interactions in lipid bilayers containing gramicidin. *Biophys. J.* **1999**, *76*, 3176−3185.

(49) May, S.; Kozlovsky, Y.; Ben-Shaul, A.; Kozlov, M. M. Tilt modulus of a lipid monolayer. *Eur. Phys. J. E* **2004**, *14*, 299−308.

(50) Siegel, D. P.; Kozlov, M. M. The Gaussian Curvature Elastic Modulus of N− Monomethylated Dioleoylphosphatidylethanolamine: Relevance to Membrane Fusion and Lipid Phase Behavior. *Biophys. J.* **2004**, *87*, 366−374.

(51) Ding, F. X.; Schreiber, D.; Verberkmoes, N. C.; Becker, J. M.; Naider, F. The chain length dependence of helix formation of the second transmembrane domain of a G protein-coupled receptor of *Saccharomyces cerevisiae*. *J. Biol. Chem.* **2002**, *277*, 14483−14492.

(52) Here, the physical basis for the nonhomogeneous lateral distribution of the membrane inclusions in the membrane is the tendency of the membrane to reach the equilibrium state, thereby minimizing the overall free energy. However, in living cells another mechanism is common: anisotropic inclusions are actively translocated to specific locations on the membrane where they can affect the preferred shape of the membrane.

(53) Iglič, A.; Kralj-Iglič, V.; Majhenc, J. Free energy of closed membrane with anisotropic inclusions. *J. Biomech.* **1999**, *32*, 1343−1347.

(54) In our calculations the free energies of outer and inner monolayers are calculated separately. In other words, except for the constraint that both monolayers are in close contact, no other interactions between the leaflets are considered. For simplicity, also the area difference between the outer and the inner monolayer is not taken into account. Calculations including the area difference between the two leaflets have been performed, yielding no significant difference in the results.

(55) Furuya, T.; Kiyota, T.; Lee, S.; Inoue, T.; Sugihara, G.; Logvinova, A.; Goldsmith, P.; Ellerby, H. M. Nanotubules formed by highly hydrophobic amphiphilic alpha-helical peptides and natural phospholipids. *Biophys. J.* **2003**, *84*, 1950−1959.

(56) Lee, S.; Furuya, T.; Kiyota, T.; Takami, N.; Murata, K.; Niidome, Y.; Bredesen, D. E.; Ellerby, H. M.; Sugihara, G. De novo-designed peptide transforms Golgi-specific lipids into Golgi-like nanotubules. *J. Biol. Chem.* **2001**, *276*, 41224−41228.

(57) Yamashita, Y.; Masum, S. M.; Tanaka, T.; Yamazaki, M. Shape Changes of Giant Unilamellar Vesicles of Phosphatidylcholine Induced

by a de novo Designed Peptide Interacting with Membrane Interface. *Langmuir* **2002**, *18*, 9638−9641.
(58) Mancini, M.; Ruckenstein, E. Lattice Site Exclusion Effect On the Double Layer Interaction. *Langmuir* **2002**, *18*, 5178−5185.
(59) Deuling, H. J.; Helfrich, W. Curvature elasticity of fluid membranes − catalog of vesicle shapes. *J. Phys. Paris* **1976**, *37*, 1335−1345.
(60) Mukhopadhyay, R.; Lim, G.; Wortis, M. Echinocyte Shapes: Bending, Stretching, and Shear Determine Spicule Shape and Spacing. *Biophys. J.* **2002**, *82*, 1756−1772.
(61) Sackmann, E. Physical Basis of Self-Organization and Function of Membranes: Physics of Vesicles. In *Structure and Dynamics of Membranes*; Lipowsky, R., Sackmann, E., Eds.; Elsevier: Amsterdam, 1995; Vol. 1.
(62) Israelachvili, J. N. *Intermolecular and Surface Forces*, 2nd ed.; Academic Press: 1992.
(63) Holthuis, J.; van Meer, G.; Huitema, K. Lipid microdomains, lipid translocation and the organization of intracellular membrane transport (Review). *Mol. Membr. Biol.* **2003**, *20*, 231−241.
(64) Corbeil, D.; Roper, K.; Fargeas, C. A.; Joester, A.; Huttner, W. Prominin: a story of cholesterol, plasma membrane protrusions, and human pathology (Review). *Mol. Membr. Biol.* **2001**, *2*, 82−91.
(65) Bruce, L. J.; Beckmann, R.; Ribeiro, M. L.; Peters, L. L.; Chasis, J. A.; Delaunay, J.; Mohandas, N.; Anstee, D. J.; Tanner, M. J. A band 3-based macrocomplex of integral and pheripheral proteins in the RBC membrane. *Blood* **2003**, *101*, 4180−4188.
(66) Gimsa, J.; Ried, C. Do band 3 protein conformational changes mediate shape changes of human erythrocytes? *Mol. Membr. Biol.* **1995**, *12*, 247−254.
(67) Baumgart, T.; Hess, S. T.; Webb, W. W. Imaging coexisting fluid domains in biomembrane models coupling curvature and line tension. *Nature* **2003**, *425*, 821−824.
(68) Kralj-Iglič, V.; Hägerstrand, H.; Veranič, P.; Jezernik, K.; Babnik, B.; Gauger, D. R.; Iglič, A. Amphiphile-induced tubular budding of the bilayer membrane. *Eur. Biophys. J.* **2005**, *34*, published online.

CI050171T